Geophysical Research Letters
December 2009 ; Volume 36 (L00D09) : Pages 1-6
http://dx.doi.org/10.1029/2009GL040820

An edited version of this paper was published by AGU.

High resolution seismic imaging of the ocean structure using a small volume airgun source array in the Gulf of Cadiz

Geli, L.[1,*], Cosquer, E.[1], Hobbs, R. W.[2], Klaeschen D.[3], Papenberg C.[3], Thomas, Y.[1], Menesguen C.[1] & Hua, B. L[1]

[1] Ifremer, BP 70, 29280 Plouzané, France
[2] University of Durham, Department of Earth Sciences, South Road, DURHAM, UK
[3] Leibniz Institute of Marine Sciences at Kiel University (IFM-GEOMAR), Kiel, Germany

*: Corresponding author : Geli L., email address : Louis.Geli@ifremer.fr

Abstract:

A small volume (117 cu-inch) seismic source producing signal predominantly in the 150–200 Hz frequency window was used during the GO calibration experiment in the Gulf of Cadiz (April–May 2007). The data show the small scale (<10 m in the z direction) internal structure of the ocean. High-resolution images display seismic reflectors that often appear as distinct, horizontal, short (~a few hundred meters to a few km long) segments, lying at different depths, while low-resolution (~20 to 30 Hz) display long, horizontal reflectors (~a few tens of km), sometimes linked by short, apparently "dipping" segments. The present data suggest that this apparent dipping effect is due to the insufficient separation power (~λ/4) of the low resolution data. Improving high resolution acquisition systems hence appears to be a critical challenge to understand the seismic response of the ocean.

Keywords: oceanography, seismics, high-resolution.

Introduction

Recent research (Holbrook et al. 2003, Holbrook & Fer, 2005, Nandi et al., 2004) has shown that the boundaries which separate water masses with different physical properties (temperature, salinity) can be successfully imaged with standard multichannel seismic (MCS) techniques. Such techniques have been commonly used for long in marine geosciences and in the oil industry to investigate the geological structure of the substratum. The energy produced by a seismic source near the sea surface is reflected at the boundaries between the water layers. For vertical incidences, the reflection coefficient (R) is equal to the impedance contrast across the boundary :

$$R(z) = \frac{d(\rho v)}{\rho(z) v(z)} \qquad (1)$$

where ρ(z) and v(z) are density and velocity at depth z, respectively. The impedance constrast R characterizes the reflectivity of the boundary. Previous studies *[e. g. Nandi et al, 2005]* have shown that impedance contrasts produced by temperature variations of a few hundredths of °C can be detected using seismic methods with a lateral resolution that is generally less than 10 m, well beyond what is usually obtained in standard oceanographic experiments.

The vertical resolution, however, is limited by the frequency content of the seismic signal (Hobbs et al., 2009) while strong reflectors near the top and bottom of Meddies (*e. g. Bower et al, 1997)*, are not produced by single interfaces but by boundary zones made of finely-scaled layers, a few meters thick (see Fig. 2). Imaging small scale (~ a few m)

structures is a critical issue for addressing fundamental questions in physical oceanography that requires high resolution seismics, particularly to determine wether energy transfer from large to small scales is a self-similar process.

The acquisition system

During the EC-Funded GO experiment different seismic sources were used to seismically image the internal structure of the Mediterranean Water Outflow at different scales in the Gulf of Cadix *(e.g. Hobbs et al., 2007, Hobbs et al., 2009).* In this paper, we present the results that were obtained with an airgun array source having a maximum usable frequency of over 250 Hz, giving at vertical resolution of less than 6 m ($\lambda/4 \approx 1.5$ m). In total 500 km of High-Resolution (HR) seismic profiles were collected (Fig. 1) together with vertical logs of the water physical properties from about 160 XBTs or XCTDs.

The seismic acquisition system was based on 6 SODERA® GI-Guns with two air chambers: the Generator (G) for producing the primary air bubble ; and the Injector (I) released after a given time delay, for limiting the primary bubble oscillation. Two sub-arrays of 3 airguns (with volumes of 24/24 and 15/15 cu-inch, respectively) spaced apart by 10 m, were towed at 1.5 meters below sea surface fired in harmonic mode, with a total generator air volume of 117 cubic inches ~ 2 liters (in comparison, the Low-Resolution (LR) source deployed during the second part of the GO experiment used a total volume of air of 2320 cu-inches ~ 38 liters).

The seismic data was recorded on a 450-m long streamer with 72 channels (group spacing of 6.25 m) and optimal towing depth at 2 m (frequency notch at 400 Hz). The weather

encountered during the cruise allows most profiles to be recorded at the optimal depth. Shots were fired every 10 s (~25 m with a ship's speed ~ 5 knots). Though in theory the optimum Common-Depth Point (CDP) spacing is 3.125 m, the CDPs have been stacked by pairs giving a spacing of 6.25m to enhance signal to noise ratio.

Data Processing

Seismic processing was specifically designed for the water column, after having muted the data from below the seafloor. The processing workflow includes : Butterworth filtering ; spatial binning; removal of the direct arrival ; NMO with water velocity 1510 m/s ; stack and migration. An example of migrated HR seismic section is shown in Figure 3. The HR acquisition system allows imaging from about 40 m to depths of about 1500 m. A consistent correlation is observed between seismic reflectors and vertical temperature gradients based on XBTs/XCTDs .

An advanced shot-gather procedure was elaborated at IFM-GEOMAR, in order to improve the efficiency of the processing by keeping the characteristic amplitude spectra of the unwanted events. The following sequence was constructed : a minimum delay filter 2/5 Hz was applied to remove non seismic events (noise), while keeping full amplitude spectra of the direct wave, back scattered tail boy waves, and reflected waves ; then, the direct wave was extracted by Karhunen-Loeve filter, followed by amplitude matching and substraction ; to remove the remaining noise created from this procedure, a high-pass zero phase filter (20/40 Hz) was applied ; then, two tau-p filters were applied to remove those steeply dipping events (tail boy noise, ship noise,...) having a broader frequency range than the main reflected events ; additional high amplitude, low-frequency events were detected in time slice mode, and filtered using a final high-pass frequency filter (30/50 Hz) ; eventually, true amplitude

common offset migration was applied with sound speed information from simultaneous oceanographic measurements (XBTs).

Post-processing (migration, spike-deconvolution) of the HR data failed to enhance the resolution at this stage. The 3-D nature of water-column reflectors seems to be more sensitive to HR data than i. e. experienced with low resolution data. The impact of moving reflector boundaries on seismic processing methods *[Klaeschen, Hill, 2009, this issue]* is not yet fully understood, but clearly complicates the migration and deconvolution, escpecially for HR data. In conclusion, the shot generated noise and the limited amount of energy produced by the small source volume results in a low signal-to-noise ratio, that demands careful pre- and post-processing to recover the weak signals. However, although low in quality (compared to LR data), only HR data provides the temporal resolution to study the effect of 'seismic oceanography' at small scales.

Filtering effect of the water column

The bandwith (50-250 Hz) of the reflection on the seabottom is centered around 150 Hz. In contrast, the bandwith of the internal reflection within the water column is centered around 100 Hz (Fig. 3). This effect maybe explained by the short-wavelength (< 5 m) internal structure of the water column, which tends to filter out the higher frequencies of the seismic signal. Let us for instance consider two different structures, one with a sharp reflectivity interface and one with a series of reflectivity interfaces, in order to represent, for instance, a velocity gradient in the water column. Reflections on sharp interfaces (simply obtained by convolving a Ricker wavelet with a Dirac-shaped reflectivity structure) have the same frequency content than the input Ricker wavelet, while reflections

on multiple interfaces may exhibit lower frequencies when the interface spacing is comparable to the wavelength of the input signal. This notch effect is particularly well illustrated in Figure 4, where the response of one reflectivity structure (with spikes, spaced every 3 m) to two different Ricker wavelets (centered on 20 Hz and 150 Hz, respectively) are compared. Unlike the solid Earth, the water does not support sharp discontinuities because diffusive effects of both heat and mass create smooth boundary zones leading to the observed loss of the higher frequency energy.

Short and flat vs longer and « dipping » reflectors

High-resolution (~150 Hz) images display seismic reflectors that often appear as distinct, horizontal, short (~a few km long) segments, lying at different depths below sea-level , while low-resolution (~ 20 to 30 Hz) often display long horizontal reflectors (~ a few tens of km) linked by short, apparently « dipping » segments. Such reflectors have sometimes been mis-interpreted as « dipping » boundaries separating different water masses apparently crossing isopycnals, but actually result from the insufficient resolving power of the low-resolution seismic data. As illustrated in Figure 5, an interface made of spatially distinct, flat segments lying at different depths may appear either as a series of flat reflectors at high-resolution, but as one single, apparently dipping, boundary at low-resolution. This is particularly important when describing the boundaries of Meddies, which are actually made of a stack of flat reflectors, a few hundreds of meters to a few kilometers long. This result confirms previous observations (Krahmann, personnal communication) based on repeated « yoyo » CTD hydrocasts made with R/V POSEIDON during time periods of 12 hours, which showed that seismic reflectors are systematically close to isopycnals.

Short scale temporal variability

Thanks to manoeuverability of the High-Resolution acquisition system, 7 sections (10 km-long each) were shot repeatedly every two hours on the continental slope (near 36°13'N, 9°10'W), showing the short-scale temporal variation of the reflectivity of the water column (Fig. 5). This variability, which could depend on tidal effects, confirms the results obtained with the « yoyo » hydrocasts, which showed an apparent vertical oscillation of the isopycnals.

Discussion

The small volume (117 cu-inch) mini GI-gun seismic source used during the GO calibration experiment provided high resolution seismic data, which, despite the low signal to noise ratio, shed new insight on the internal structure of the ocean. Improving the S/N ratio of high resolution seismics appears to be a challenge of critical importance, not only to image the small scale (~ a few m in z) structures, but also to help understand the seismic images that we presently have from the ocean.

To reach this challenge, one cannot play on the fold coverage by increasing the length of the streamer, due to the filtering effect of the receiver at large incidence angles. At frequencies > 175 Hz, the antenna effect is such that the amplitude of the seismic signal is divided by a factor of two at incidence angles greater than ~ 60° : so the amplitude of the reflections from the shallowermost interfaces decreases rapidly as the source-receiver offset increases.

The solution consists in increasing the seismic energy emitted in the water column. Seismic airguns produce their acoustic radiation by the release of high pressure gases into the water. The acoustic energy output is a complex relationship between the physical shape of the gun, the air-pressure, the chamber volume, the ambient temperature and hydrostatic pressure *[Parkes and Hatton, 1986]* . The bubble period T and amplitude A of the pulse emitted by one a single gun of volume V increases as $V^{1/3}$ when the pressure and depth are held constant : the higher the frequency of the pulse, the smaller the volume of the source and the smaller the amplitude of the seismic signal. So the optimum design to improve the signal to noise ratio require arrays with a very large number of small volumes gun, as this is a more effective means to increase output energy over simply increasing the volume. The high-frequency characteristics can be further improved by the use of GI or mini GI guns as used here as these suppress the bubble pulse giving an improved impulsive source. Another solution could be to design a broad-band system as proposed by *[Hobbs et al [2009]*, with sources and receivers towed at different depths.

Conclusions

By using high-frequency a seismic source we have been able to image the fine-scale water structure down to a vertical resolution compatible with CTD casts and a horizontal resolution of 6.25m. This has revealed new insights into the spatial nature of boundaries in the water layer. In particular the evidence that boundaries tend to form along isopycnals. If the interface between two water masses is inclined then the reflectors form a shingled staircase of short sub-horizontal events. Previous seismic imaging of these boundaries using low-resolution systems had produced evidence of « dipping » events. From a simple model and from direct

observation of the boundaries of a Meddy in the Gulf of Cadiz, we conclude that these effects result from the seismic acquisition system.

Acknowledgments : *The GO project was funded by the 7th Framework Programme for Research and Development of the European Community. The captain and crew of R/V Discovery are greatly acknowledged. The authors of the present paper wish to thank all other partners that made the GO project a success, particularly Gerd Khrahmann, who made possible the use of R/V Poseidon with support of the German Science Foundation. of acquisition parameters. Help from Frauke Klingelhoefer, Bruno Marsset, Elise Quentel, Ekaterina Vserminova, Laetitia Morvan, Estelle Théréau is also acknowledged. Careful reviews helped improve the manuscript.*

REFERENCES

Bower A.S., Armi L., Ambar I., Lagrangian observations of Meddy formation during a mediterranean undercurrent seeding experiment, *Journal of Physical Oceanography, 27, pp. 2545-2575, 1997.*

Holbrook W.S., Fer I., Ocean internal wave spectra inferred from seismic reflection transects, *Geophysical Research Letters, 32, 2005.*

Hobbs, R. W., Hobbs R.W. PROJECT: GO – Geophysical Oceanography: A new tool to understand the thermal structure and dynamics of oceans. *European Union Newsletter* **2:7**. Available online at: www.aapg.org/europe/newsletters/2007/06jun/06jun07europe.pdf, 2007

Hobbs, R. W., Klaeschen, D., Vserminova, E., Papenberg, C., The effect of seismic source bandwith on reflection sections to image water structure, *Geophys. Res. Let.*, this issue, 2009

Holbrook W.S., Paramo P., Pearse S., Schmitt R.W., Thermohaline fine structure in an oceanographic front from seismic reflection profiling, *Science, 301, pp. 821-824, August 2008.*

Klaeschen D., Hill, D., Moving reflectors and seismic processing in the water column, *Geophys. Res. Let.*, this issue, 2009

Nandi P., Holbrook W.S., Pearse S., Paramo P., Schmitt R.W., Seimic Reflection imaging

of water mass boundaries in the Norwegian Sea, *Geophysical Research Letters, 31, 2004.*

Parkes G., & Hatton, L., The marine seismic source, *D. Reidel Publishing Company, Kluwer Academic Publishers*, 184 pp, 1986

FIGURE CAPTIONS

Figure 1 : Implementation of the HR seismic lines collected during the GO experiment in April/May 2007 in the Gulf of Cadix.

Figure 2: Seismic image of a meddy along profile LR01 obtained with R/V Discovery during the second leg of the GO experiment (may 2007) using a standard, low-resolution source of 2320 cu-inches producing signal with predominant frequencies in the 20 – 30 Hz window. This section overlaps with Line HR-018 shown in Figure 1, but was shot two weeks later. The yellow line indicates the location of CTD 10, collected with R/V Poseidon as seismic data was acquired. Reflectivity may be directly computed based on the CTD data, using Formula (1). Theoretically, the derivative expressed in Formula (1) is valid when dz tends to zero. In practise, however, dz depends on the sampling rate available along a vertical column. In the present case, the CTD data has been resampled at 1m in order to avoid short wavelength noise, so dz=1m. The right part of the figure represent Seawater Temperature, Reflectivity and synthetic seismogram in response to Ricker wavelets at dominant frequency of 20 Hz and 150 Hz in, respectively, the [0.8 – 1.1] and [1.7-2.0] seconds two-way travel-time (s-twt) windows. This figure clearly shows that the strong reflectors at the top and at the bottom of the meddy are not related to sharp interfaces. Instead, they are related to transition zones made of small-scale layers, less than ~ 5 to 10 meters thick.

Figure 3 : Migrated High resolution seismic line HR-10 obtained with the small volume source of 117 cu-inch described in the text. Automatic Gain Control is applied, producing an artificial blank above seabottom. The wavelet extracted from the sea-bottom reflection

exhibits a spectrum with predominant frequencies in the [150 – 200] Hz window (insets a to d). In contrast, the wavelet extracted from the reflector in the water column (insets e and f) is characterized by lower frequencies, predominantly in the [50 – 130 Hz] window, suggesting that the small-scale internal structure of the ocean produces a low-pass filter effect.

Figure 4 : Simple modelling to explain the filtering effect due to the internal structure of the water column. The responses of a layered structure (modelled by 5 reflectivity spikes, spaced by 3 meters apart) to two different Ricker wavelets (of 20 and 150 Hz, respectively) are compared. Note that the layered structure acts as a low-pass filter, producing a notch effect on the 150 Hz response spectrum.

Figure 5 : HR image (lines 30-31) of a meddy, showing signal down to 1.5 – 2 s-twt. Main boundaries are made of a series of short, flat reflectors, that may appear as « dipping reflectors » when imaged with low resolution seismics. Insets c and d show the seismic response of a staircase structure to Ricker wavelets at 150 and 20 Hz respectively (vertical stair spacing is here equal to 7.5 m). It is important to highlight that the « dipping » effect is not totally an artifact, as infinite horizontal layers would not produce dipping reflectors. The reflectors appear as « dipping » because the boundary consist in a staircase made of sharp interfaces of limited horizontal extent.

Figure 6 : High-resolution seismic sections, shot repeatedly every four hours from the SW to the NE, on the continental slope (near 36°13’N, 9°10’W), showing the short-scale temporal variation of the water column.

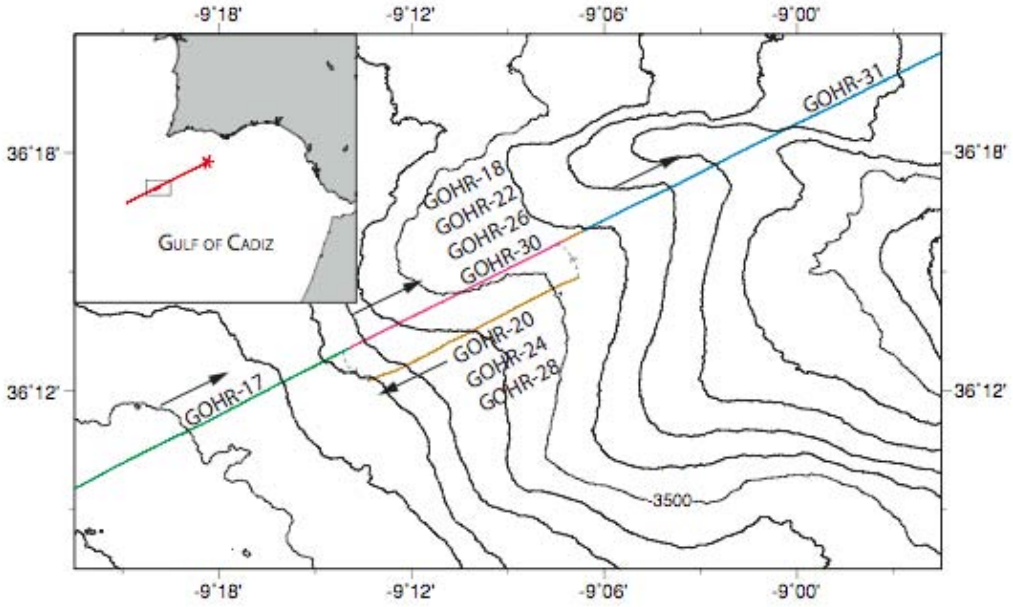
-9°18'
-9°12'
-9°06'
-9°00'
36°18'
36°12'
GULF OF CADIZ
GOHR-31
GOHR-18
GOHR-22
GOHR-26
GOHR-30
GOHR-20
GOHR-24
GOHR-28
GOHR-17
-3500

FIGURE 1

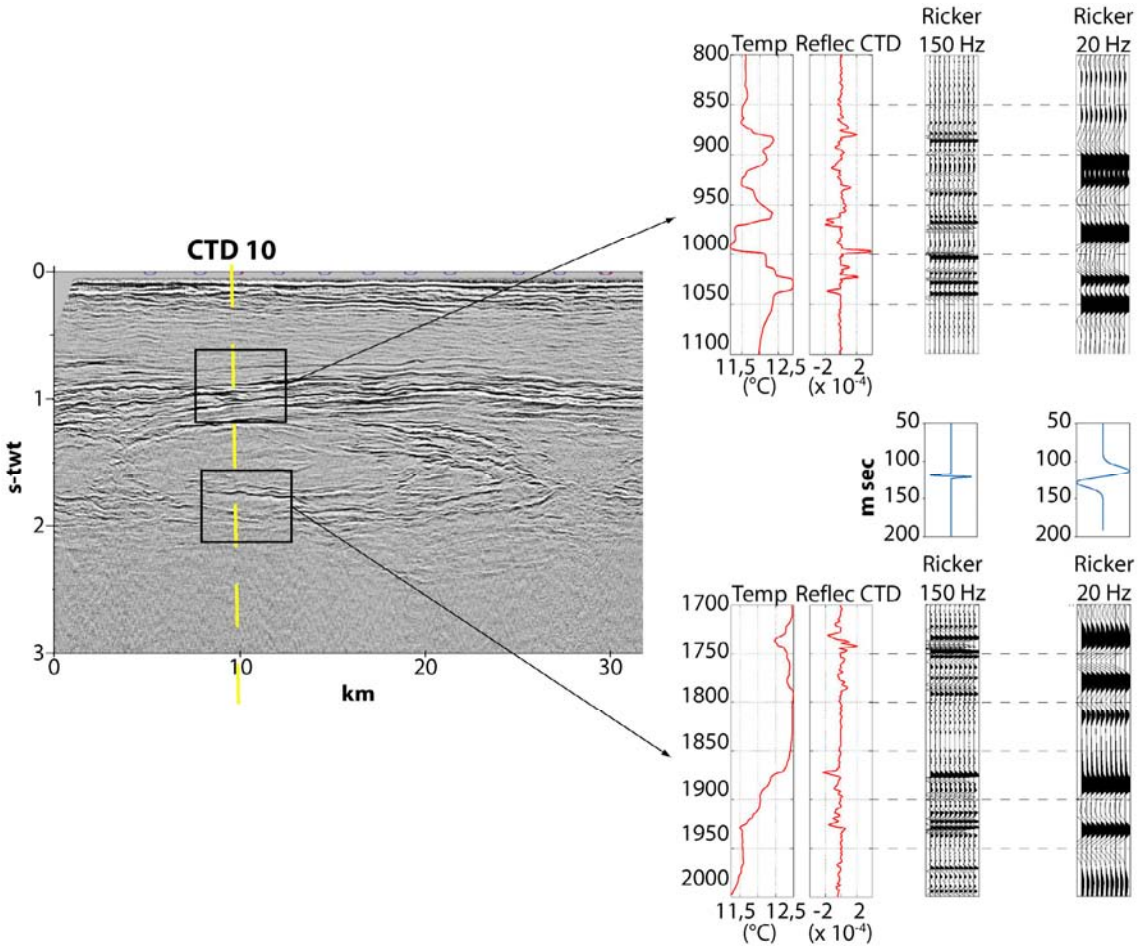
CTD 10
s-twt
km
Temp
Reflec CTD
Ricker 150 Hz
Ricker 20 Hz
(°C)
(x 10⁻⁴)
m sec

FIGURE 2

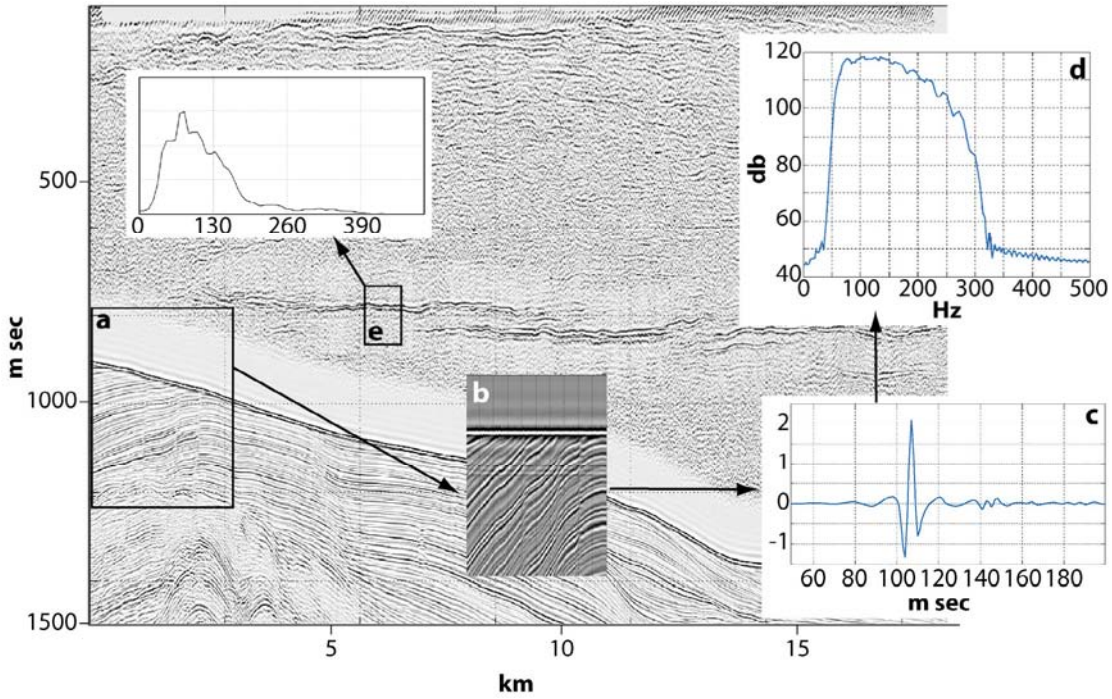
500
1000
1500
m sec
5
10
15
km
a
b
c
d
e
0
130
260
390
120
100
80
60
40
db
0
100
200
300
400
500
Hz
2
1
0
-1
60
80
100
120
140
160
180
m sec

FIGURE 3

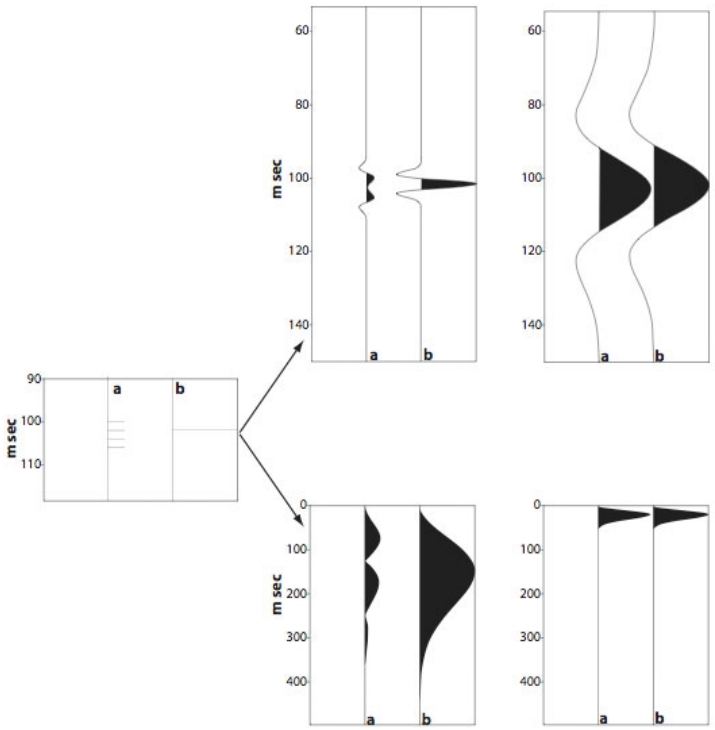
90
100
110
m sec
a
b
60
80
100
120
140
m sec
a
b
60
80
100
120
140
a
b
0
100
200
300
400
m sec
a
b
0
100
200
300
400
a
b

FIGURE 4

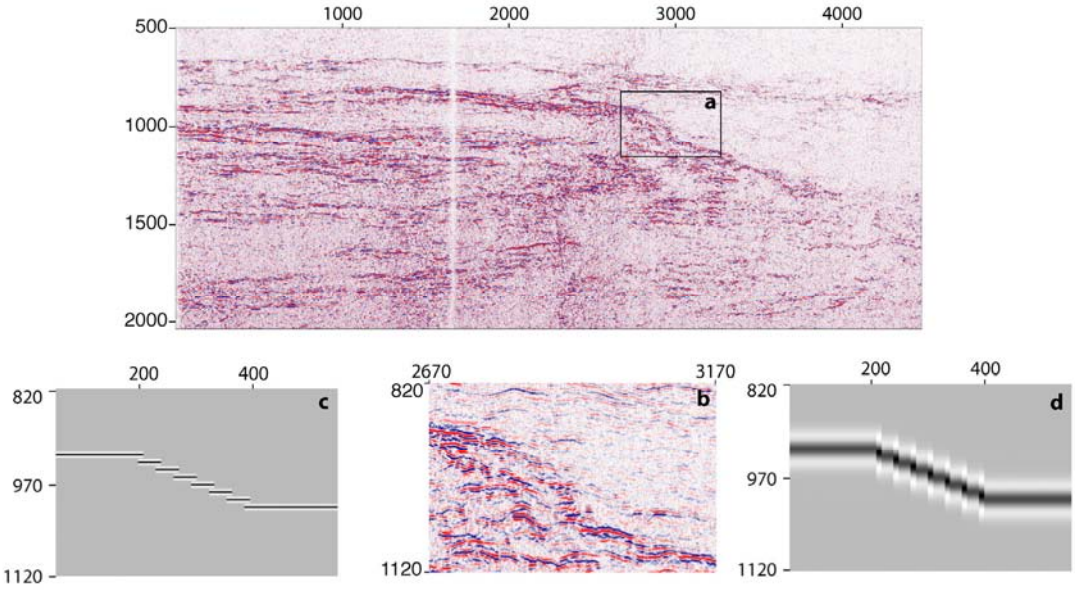
1000
2000
3000
4000
500
1000
1500
2000
a
200
400
820
970
1120
c
2670
3170
820
1120
b
200
400
820
970
1120
d

FIGURE 5

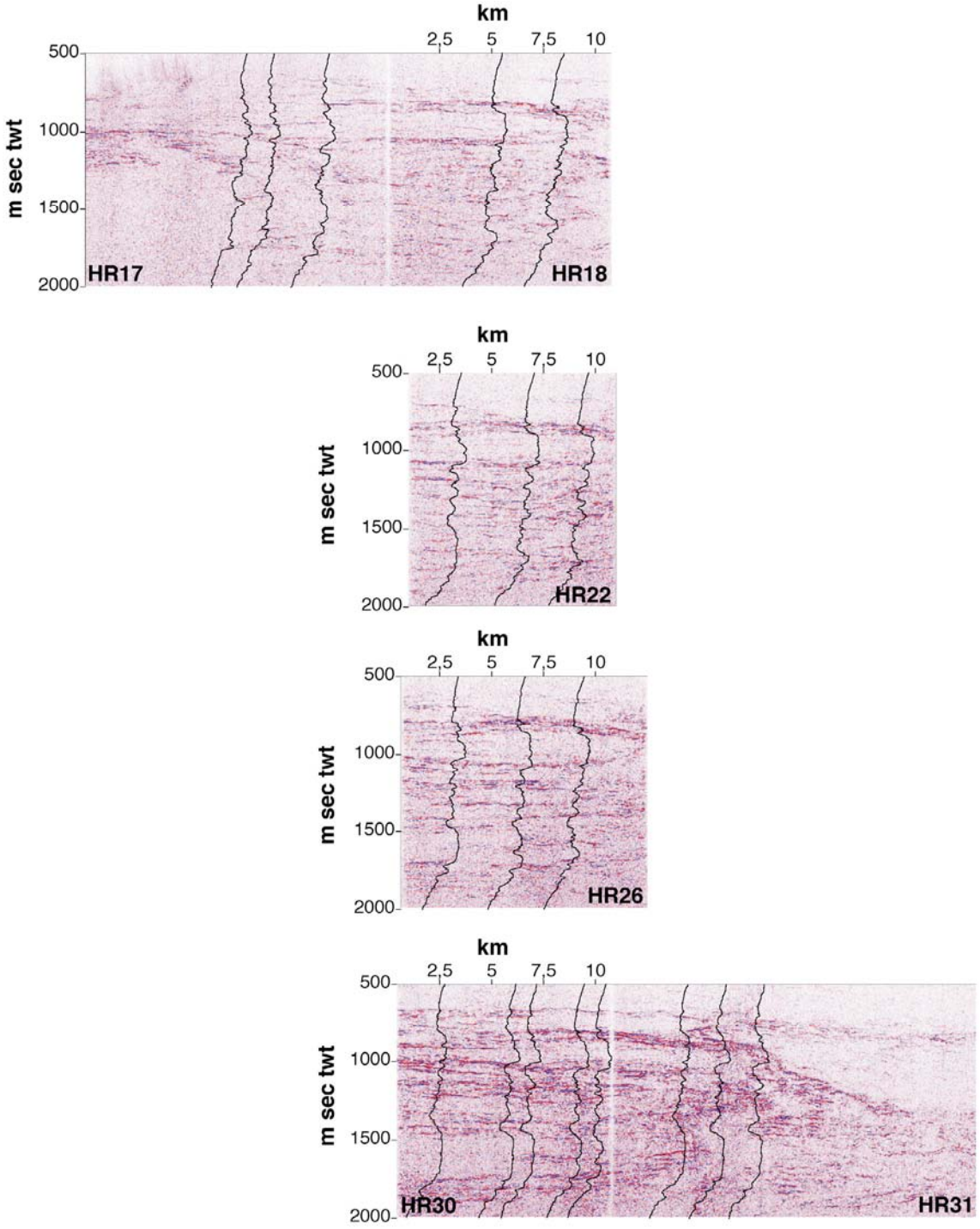
km
2,5
5
7,5
10
500
1000
1500
2000
m sec twt
HR17
HR18
HR22
HR26
HR30
HR31

FIGURE 6

The internal structure of reflectors : a wavelet analysis

Because seismic traces reflect oscillatory phenomena, seismograms have a zero-sum, hence wavelet analysis can be successfully applied to produce an estimate of the frequency content at different depths in the dataset (a correspondance is made between the depth below sea surface z, and the propagation time of the seismic wave, t, assuming a vertically averaged seismic velocity equal to 1510 m/s). Wavelet analysis is based on the convolution of the function to analyze -f(u)- with a set of functions derived from a mother wavelet g(u), as follows :

$$T_g(b,a) = \frac{1}{\sqrt{a}} \int g\left(\frac{u-b}{a}\right) f(u)du \qquad (A1)$$

$T_g(b,a)$ is known as the continuous wavelet transform of f, *a* (>O) and *b* are real numbers that may be varied continuously. Because seismic traces reflect oscillatory phenomena, the seismograms have a zero-sum and wavelet analysis can be successfully applied. Translation parameter *b* then corresponds to position, and dilation parameter *a*, to scale length. Equation (A1) expands a one-dimensional depth series into the two-dimensional parameter space (*b*, *a*) and yields a local measure of the relative amplitude of activity at scale *a* at depth *b*. In the general case, there is no straightforward relationship between the scale *a* of the wavelet transforms and the wavenumber *k* of the Fourier modes wavelength *[e.g. Meyers et al, 1993]*. However, here, we have used the Morlet wavelet *[Morlet, 1983]*, so that a linear relation is obtained between wavelet scale *a* and Fourier wavelength λ (see the Appendix in *[Meyers et al, 1993]).* In the computer program that we have used *[Torrence and Compo, 1998 ; Grinsted et al, 2004]*, a « Fourier correction factor » is systematically applied, so that the words « wavelet scale » and « Fourier wavelength » indistinctly. Eventually, the χ^2–test (with

a threshold of 95%) was applied to the results in order to determine the statistical significance of the wavelet characteristics [Greenwood and Nicolin, 1996]. The wavelet transform characteristics (in terms of wavelength and amplitude) are accepted as « significant » if they comply with the χ^2–test, that is : the probability that such characteristics result from a random process is less than 5%.

The wavelet analysis was performed on the seismograms, but also on the synthetic reflectivity profiles using the *in-situ* temperature (T) and salinity (S) measurements collected during the GO-cruise (the smooth trend of T and S was removed in order to obtain « de-trended » functions, $T_d(z)$ and $S_d(z)$, with zero sum and finite L2-norm, allowing the wavelet transform analysis). The results (Fig. A1) confirm that strong reflectors display significant energy also at wavelengths < 10 m, suggesting that the major boundaries, particularly those near the top and near the base of meddies, are made of stacked layers, a few meters thick.

References

Greenwood P. and Nikulin, P., A guide to Chi-squared testing, *John Wiley and Sons (Book Publishers)*, 1996

Grinsted, A., S. Jevrejeva, J. Moore, "Application of the cross wavelet transform and wavelet coherence to geophysical time series." *submitted to a special issue of Nonlinear Proc. Geophys., 'Nonlinear analysis of multivariate geoscientific data - advanced methods, theory and application'*, 2004.

Meyers, S. D., Kelly, B. G., and O'Brien, J. J., An introduction to wavelet analysis in oceanography and meteorology : with application to the dispersion of Yanai Waves, *Monthly Weather Review*, 121, 2858-2866, 1993

Morlet, J., Sampling theory and wave propagation. *NATO ASI Series. 1. Issues in Acoustic Signal/Image Processing and Recognition* ; *Chen, C. H.. Ed. Springer*, 233-26, 1983

Torrence, C., and G.P. Compo, A practical guide to wavelet analysis, *Bull. Am. Meteorol. Soc., 79, 61-78, 1998.*

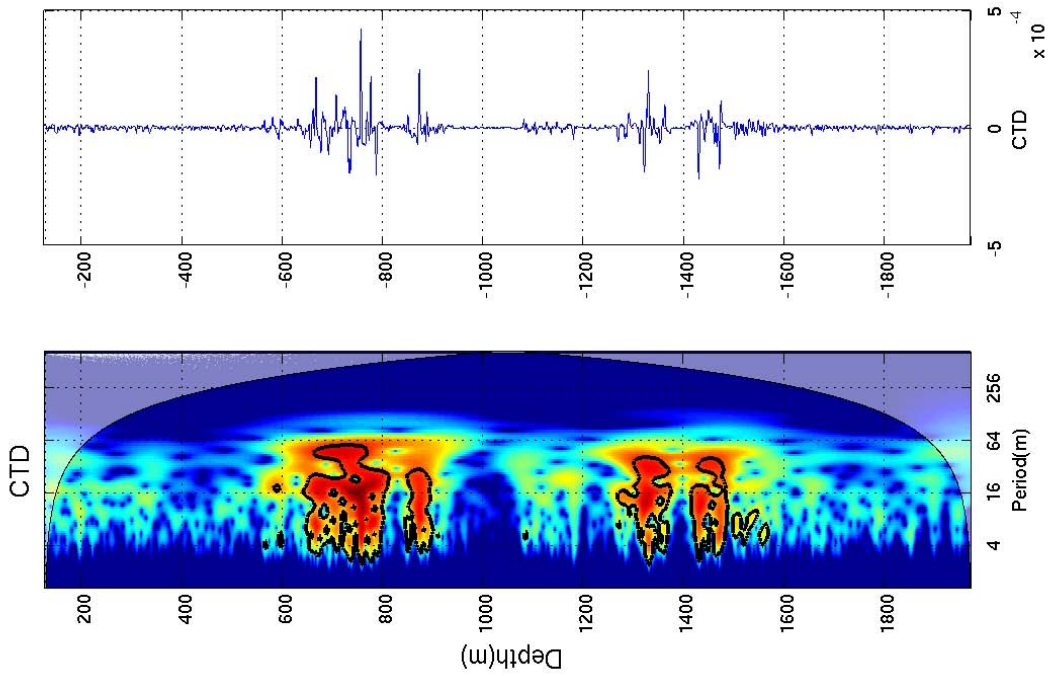

Fig. A1. Top : Synthetic reflectivity based on the T and S measurements from CTD profile number 42, collected with R/V Poseidon during the second part of the GO Experiment along seismic Line LR01. Bottom. Wavelet analysis of the reflectivity, as explained in the text. The strong amplitudes between 600-900 m and between 1300-1500 m are related to the reflectors located near the top and bottom of a meddy. The boundaries of meddies are made of stacked layers, a few meters thick, that would require high resolution seismics to be fully imaged.